Coating of 2-Aminobenzimidiazole and 1-(o-Tolyl)biguanide Functionalized Silicas on Iron Sand Magnetic Material for Sorption of $[AuCl_4]^-$

Nuryono[1,*], Nur Mutia Rosiati[1], Abraham L. Rettob[2], Suyanta[1], and Yateman Arryanto[1]

[1]*Department of Chemistry, Faculty of Mathematics and Natural Sciences, Universitas Gadjah Mada, Sekip Utara, Yogyakarta 55281, Indonesia*

[2]*Faculty of Teachers Training and Education, Musamus University, Jl. Kamizaun Mopah Lama, Merauke 99600, Indonesia*

Corresponding author:

email: nuryono_mipa@ugm.ac.id

Received: April 11, 2018
Accepted: July 26, 2018

DOI: 10.22146/ijc.34653

Abstract: *Two novel materials of 2-aminobenzimidiazole (AB) and 1-(o-tolyl)biguanide (TB) modified silicas coated on the iron sand magnetic material (MM@SiO_2/AB and MM@SiO_2/TB) have been synthesized and were used to adsorb Au(III) from Au/Cu/Ni solution. Silica layering MM was modified with polyamino compounds via a sol-gel process using a sodium silicate solution, 3 chloropropyl trimethoxysilane (CPTS) and modifier compounds. Adsorption of Au(III) on MM@SiO_2/AB and MM@SiO_2/TB was investigated in a batch system by varying pH, initial concentration, contact time and the presence of other metal ions (Cu(II) and Ni(II)). The results showed that MM@SiO_2/AB and MM@SiO_2/TB were successfully synthesized through the sol-gel process using cross-linking agent CPTS. Adsorption of Au(III) on MM@SiO_2/AB and MM@SiO_2/TB decreased with the increase of pH and followed the Langmuir isotherm models with adsorption capacity of 17.15 and 9.44 mg/g, respectively. The adsorption kinetics fit to a pseudo-second-order model with the rate constants of 1.16 × 10^{-2} and 1.46 × 10^{-2} g mg^{-1} min^{-1}, respectively. MM@SiO_2/AB and MM@SiO_2/TB gave a high selectivity towards Au(III) in a mixture of Cu(II) and Ni(II). The desorption using thiourea 1 M solution in 1 M HCl of metal ions showed that percentage of Au(III) desorbed was higher than that of Cu(II) and Ni(II).*

Keywords: *adsorption; iron sand; aminobenzimidiazole; tolylbiguanidine; gold*

■ INTRODUCTION

It is well known that gold (Au) exhibits many special characters and high economic value. Currently, the use of gold is not only as jewelry but also can be used in various fields, such as catalysis [1] and the electronic industry as components of Printed Circuit Board (PCB) [2-4]. The growth of the electronic industry leads to the increase of gold used in this field and the amount of electronic waste in the environment. The electronic components are not only gold but also other metals such as copper, zinc, and nickel. Consequently, a simple and efficient method for gold separation from other metals is required.

One of the gold separation methods as an ion, Au(III), is adsorption which has many advantages, including environmental-friendly, no hazardous waste, inexpensive, can be applied at a low concentration of metal ion [5] and the adsorbent can be used repeatedly [6]. Various types of adsorbents can be used in the process of Au(III) adsorption, such as nanoporous adsorbents [7], nanofiber membranes [8] and modified silica [5,9-11]. However, adsorption using this type of adsorbent is usually time-consuming in separation between adsorbent and filtrate.

One attempt to improve the effectiveness of silica-based materials as an adsorbent of Au(III) and other metal ions is by modifying it using organic functional groups [10]. The previous researcher proved that the functional groups of amines, monoamine, diamine or triamine are able to be used to modify the silica surface and to be used as a heavy metal adsorbent [5]. The amino groups can act as an electron-pair donor to the metal ions. As a result, the amine group is able to adsorb metal

ions [10-12]. The results showed that the adsorption capacity of Cu(II), Ni(II), Pb(II), Cd(II), and Zn(II) increases with increasing nitrogen atom number in the adsorbent [5]. However, the number of amino groups per molecule of modifying compound seems not significantly affect the adsorption capacity for Au(III). Sakti et al. [11] reported that the capacity of silica modified with aminopropyl silane to adsorb Au(III) was 134 mg/g, while silica modified with arginine adsorbed 53 mg/g [12]. It seems that the environment of active sites including the presence of phenyl around the amino groups influences the capability in binding Au(III). Thus, two compounds containing both phenyl and amino groups namely 2-aminobenzimidazole (AB) and 1-(o-tolyl)biguanidine (TB) (Fig. 1) are investigated.

■ EXPERIMENTAL SECTION

Materials

Iron sand magnetic material (MM) was separated from Iron sand collected from Bugel Beach, Kulonprogo, Yogyakarta, Indonesia referring to the procedure reported by Fahmiati et al. [18]. Ten grams of iron sand sample was separated using the external magnetic field to obtain MM. The attracted MM was sieved to 70 meshes and then washed with distilled water and dried at 80 °C. The MM was soaked with 10% HF solution and sonicated for 15 min. The soaked MM was washed with distilled water and was dried at 80 °C. The MM obtained was 81.6% of iron sand treated. Chemicals used for coating MM were purchased from Merck including Na_2SiO_3 solution (7.5–8.5% Na_2O and 25.5–28.5% SiO_2), 3-chloropropyltrimetoxisilane (CPTS) and NaCl, and 2-aminobenzimidazole (AB) and 1-(o-tolyl)-biguanidine (TB) were supplied from Aldrich. Metal ions used for adsorption experiments were originated from $HAuCl_4$, $NiCl_2{\cdot}6H_2O$, and $CuCl_2{\cdot}2H_2O$ (Merck) dissolved in 1 M HCl solution, and chemicals for desorption were thiourea solution in 1 M HCl.

Instrumentation

Fourier Transform Infrared (FTIR) Spectrophotometer (Shimadzu FTIR Prestige 21), X-ray Diffractometer (XRD) (Rigaku Multiflex), Vibrating Sample Magnetometer (VSM) (VSM Oxford 1,2 T) were used to identify the presence of the functional groups, crystallinity, and magnetism, respectively. Atomic Absorption Spectrophotometer (AAS) (Analytic Jena contrAA 300) was used for analyzing Fe dissolved during stability test of products and the un-adsorbed metal ions.

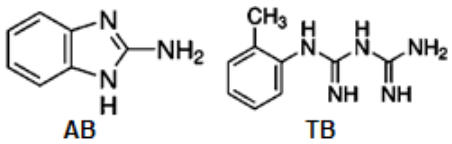

Fig 1. Structure of 2-aminobenzimidazole (AB) and 1-(o-tolyl)biguanidine (TB)

Procedure

Coating of MM and its characterization

About 0.5 g of MM was activated with 1 mL of 1 M HCl solution and the activated MM was added with 1 mL of sodium silicate solution to obtain Mixture 1. Mixture 2 was prepared by mixing 1.8 mL of CPTS, 6 mL of DMF and modifiers (1.28 g of AB or 1.83 g of TB). Mixture 2 was poured into Mixture 1 and then was added with 1 M HCl solution dropwise to form a gel. The formed gel was kept overnight and then dried in an oven at 80 °C for 4 h. The dried product was grounded, washed with distilled water, and dried at 80 °C for 4 h. The obtained product was characterized by FTIR spectrophotometer, XRD, VSM. Besides, acidic stability was tested at various pHs, and pH_{PZC} was determined.

The acidic stability was carried out by mixing 10 mg of samples and 10 mL pH buffer solution at various pHs (1-6) prepared using HCl solution, $C_6H_8O_7{\cdot}H_2O$, and $Na_3C_6H_5O_7{\cdot}2H_2O$. The mixture was shaken for 60 min and the filtrate was separated with an external magnetic field. The dissolved Fe ion was analyzed with AAS.

The pH_{PZC} value of coated MM sample was determined by adjusting pH of 0.01 M NaCl solutions using 0.1 M HCl or 0.1 M NaOH solution to reach pHs of 1–10. About 10 mg of coated MMs was put into each container of NaCl solution with different pH. The mixtures were shaken for 60 min, kept for 3 days and then the final pH was measured.

Adsorption of metal ions

Adsorption was carried out in a batch system by adding 10 mg of adsorbent in 10 mL of buffer solution containing Au(III) 50 mg/L. The mixture was stirred for 1 h and the adsorbent was separated with an external magnet. The amount of Au(III) not adsorbed was analyzed with AAS, and the adsorbed Au(III) was calculated using Eq. (1):

$$Q = \frac{(C_0 - C_e)V}{w} \quad (1)$$

where Q represents the amount of Au(III) adsorbed (mg g^{-1}); C_0 and C_e are the initial and the final concentrations of the metal ion (mg L^{-1}), respectively; W is the mass of the adsorbent (g), and V is the volume of the metal ion solution (L).

The pH was adjusted and varied from 1.0 to 6.0. An analog work of the adsorption was performed by varying the Au(III) concentration, in a range of 5–75 mg/L, at optimum pH. The resulted data was evaluated using Langmuir and Freundlich isotherm models. In addition, adsorption in various contact times (15–240 min) at optimum pH and Au(III) concentration was conduct and the kinetics were studied using models of pseudo-first-order and pseudo-second-order. Adsorption of Au(III) in the presence of other metal ions, Cu(II) and Ni(II), was also conducted. About 10 g coated MM was mixed with 10 mL metal ion mixture of Au(III)/Cu(II)/Ni(II) with the various concentration ratios of Au(III) (20 mg/L) to other metal ions (20, 40, and 60 mg/L). The adsorption selectivity of coated MM to Au(III) was presented as a selectivity coefficient of Au(III) to another ion M ($\alpha_{Au/M}$) calculated using Eq. (2).

$$\alpha_{Au/M} = \frac{D_{Au}}{D_M}, \; D = \frac{Q}{C_e} \quad (2)$$

where D represents the distribution coefficient of ion, Q is capacity and C_e concentration of ion at equilibrium.

Desorption of metal ions

Amount of 10 mg adsorbent was put into a bottle containing of Au(III), Cu(II), Ni(II) with various concentrations ratios (Au(III):Cu(II):Ni(II) = 20:0:0; 20:20:20; 20:40:20 and 20:20:40 mg/L) and then shaken for 60 min. The adsorbent was separated with an external magnet and the filtrate was analyzed using AAS. The adsorbent was dried at 40 °C and then 10 mL thiourea 1 M in 1 M HCl solution added into it and shaken for 60 min. The adsorbent was separated with an external magnet and the filtrate was measured by AAS.

■ RESULTS AND DISCUSSION

Characteristics of MM@SiO_2/AB and MM@SiO_2/TB

Functional groups

The presence of functional groups in the products has been identified based on the IR spectra as presented in Fig. 2. From the figure seems that stretching vibration of M-O-M (M = Si or Ti) is observed at 1041–1057 cm^{-1}. The absorption band at 3448 cm^{-1} appears from stretching of –OH bond [18].

Vibration band at 571 cm^{-1} comes from the absorption of Fe-O bond [15]. The intensity of this peak decreases after MM coating. This is due to the presence of layer on MM surface. The appearance of the band at 463-471 cm^{-1} indicates the presence of Si-O-Si. Stretching vibration of Si-O-Si is observed at 787–802 and 1039–1088 cm^{-1}. Stretching vibration of Si-OH is identified at 910–941 cm^{-1} [19]. The absorption bands at 1628–1636 and 3418–3449 cm^{-1} in coated MM spectra come from bending and stretching of -OH in Fe-OH and Si-OH.

Using 3-chloropropyltrimetoxisilane (CPTS) as a cross-linking group between silica and functional groups causes the presence of absorption band from bending of -CH_2- at 1442 cm^{-1}. The absorption band at

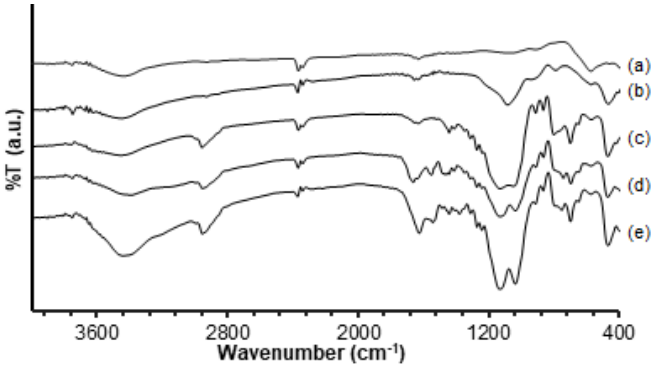

Fig 2. FTIR spectra of (a) MM after activation with HF, (b) MM@SiO_2, (c) MM@SiO_2/CPTS, (d) MM@SiO_2/AB and (e) MM@SiO_2/TB

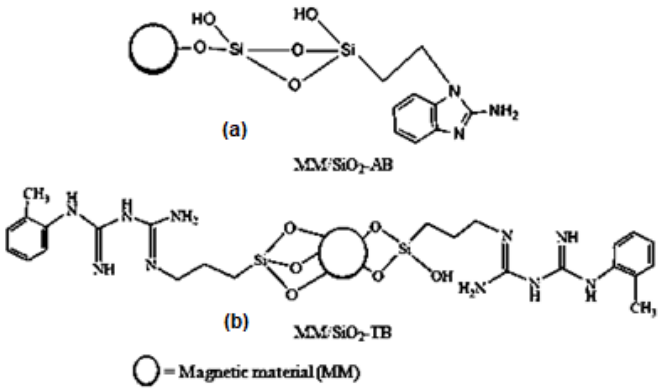

Fig 3. Structural model of (a) MM@SiO_2/AB and (b) MM@SiO_2/TB

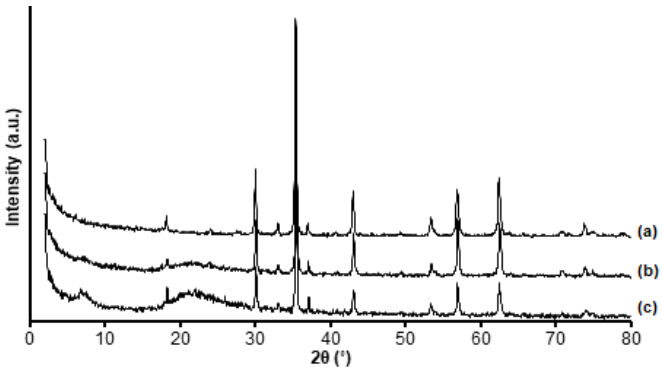

Fig 4. XRD patterns of (a) MM after activation with HF, (b) MM@SiO_2/AB and (c) MM@SiO_2/TB

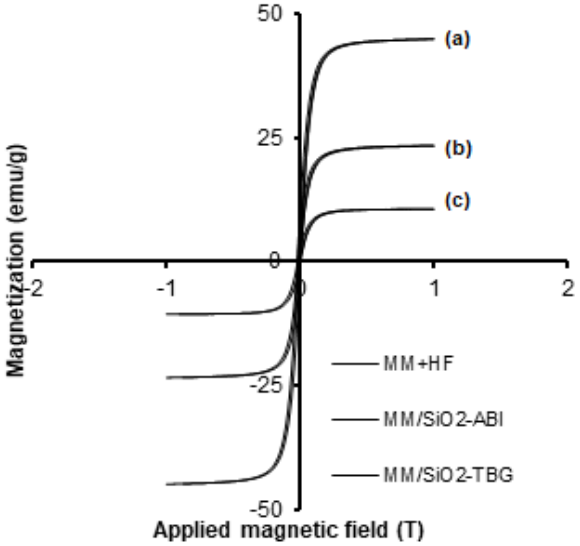

Fig 5. The magnetization hysteresis loop of (a) MM after activation with HF, (b) MM@SiO_2/AB and (c) MM@SiO_2/TB

1126 cm^{-1} is identified from stretching of Si-CH_2. The presence of C-H results in absorption band at 2955 cm^{-1} as asymmetric stretching vibration [19]. Therefore, those peaks are not detected on MM and MM/SiO_2.

The appearance of C=C benzene aromatic ring stretching vibration band at MM@SiO_2/AB indicates that AB ligand was successfully coated on MM. This is evidenced by the presence of C=N stretching vibration band of the imidazole ring at 1558 cm^{-1}. The observed bands around 3300 cm^{-1} correspond to stretching of –OH and –NH [15].

The success of coating with TB to form MM@SiO_2/TB was proved by the presence of C-N stretching vibration at 1381 cm^{-1}. Stretching vibration of the C=C benzene ring is detected at 1543 cm^{-1}. This band coincides with the absorption band of C=N stretching. The absorption band at 1628 cm^{-1} derived from multiple vibration bands; –OH, -NH and C=C aromatic. The presence of a band at 3426 cm^{-1} originates from the stretching of –OH and –NH [15]. The FTIR analysis results show the presence of Fe-O, Si-C, C-N and Si-O-Si bonds. This may form the structure model of MM@SiO_2/AB and MM@SiO_2/TB as presented in Fig. 3.

Crystallinity

The XRD patterns of uncoated and coated MMs are shown in Fig. 4. It describes the type of iron oxide containing in MM. The iron oxide dominant phase of MM is magnetite according to Powder Diffraction File (PDF) No. 19-0629. Silica iron oxide ($Fe_{2,95}Si_{0,05}O_4$) according to PDF No. 52-1140, titania iron oxide ($(Fe_{2,5}Ti_{0,5})_{1,04})O_4$) according to PDF No. 51-1587 and ilmenite (Fe_2TiO_3) according to PDF No. 29-0733 are also detected. The decrease of MM diffraction peaks intensity and the appearance of new peaks are observed after coating

Table 1. Magnetic properties of uncoated and coated MM

Material	M_s (emu/g)	M_r (emu/g)	H_c ($\times 10^{-2}$ T)
HF treated MM	44.90	10.90	1.69
MM@SiO_2/AB	23.30	5.41	1.93
MM@SiO_2/TB	10.60	2.23	1.86

of MM with silica hybrid. The presence of broad peaks at 6.04 and 20.48° on coated MM XRD patterns indicate that MM has been successfully coated with silica [20].

Magnetism

Magnetic properties of bare MM and coated MM were measured at room temperature and the results are shown in Fig. 5. It reveals that coating of MM reduces the maximum saturation magnetization (M_s) of MM from 44.90 emu/g to 23.30 emu/g for MM@SiO_2/AB and to 10.60 for MM@SiO_2/TB, as presented in Table 1.

It is probably due to the presence of layer on MM surface while these silica hybrid layers have no magnetic property [6,14,21]. A lower M_s value of MM@SiO_2/TB may be explained because of a higher molecular weight of TB that leads slower response of MM@SiO_2/TB to the external magnetic field than that of MM@SiO_2/AB.

Stability in acidic condition

The stability test of adsorbents at various acidic pHs is evaluated for detecting the amount of Fe ions dissolved from coated MM. The decrease of Fe content in MM may reduce the magnetic properties of adsorbent. Fig. 6 shows that dissolved Fe ions from coated MM are not more than 2.5%. The insignificant difference of the dissolved Fe at various acidic pHs indicates that MM@SiO_2/AB and MM@SiO_2/TB are stable at these acidic pHs so these adsorbents could be used for adsorption in these pHs range.

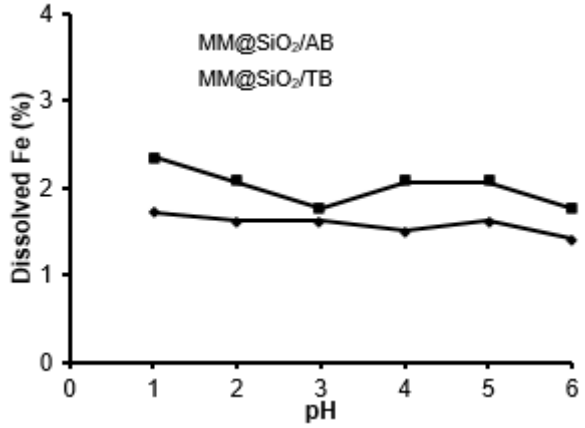

Fig 6. The effect of pHs to dissolved Fe (%) of MM@SiO_2/AB and MM@SiO_2/TB

pH_{PZC} value

Value of pH_{PZC} was investigated to determine the type of adsorbent surface charge at a certain pH. The increase of solution pH corresponds to the protonated functional groups on the adsorbent surface so that is charged positively. On the other hand, if the final solution pH is lower than initial solution pH, it indicates the increase of H^+ ions in solution. This phenomenon proves the occurrence of functional groups deprotonation on the adsorbent surface. Fig. 7 shows that pH_{PZC} of MM@SiO_2/AB is obtained to be around 5.4 while that of MM@SiO_2/TB is found at 5.9. Therefore these adsorbents are positively charged below these pHs.

These values are lower than pH_{PZC} of bare magnetite which is found to be around 8.2 [21], indicating MM were covered by silica hybrid. A higher pHpzc value of MM@SiO_2/TB than that of MM@SiO_2/AB could be expected since the number of amine groups on TB ligand is more than it on AB ligand. Therefore the amount of H^+ ions required for protonating active sites of the adsorbent surface on MM@SiO_2/TB is higher than it on MM@SiO_2/AB.

Adsorption

Effect of pH on Au(III) adsorption

To investigate the effect of pH on Au(III) adsorption, the adsorption was done at various pH from 1.0 to 6.0. The reduction tendency of adsorption capacity

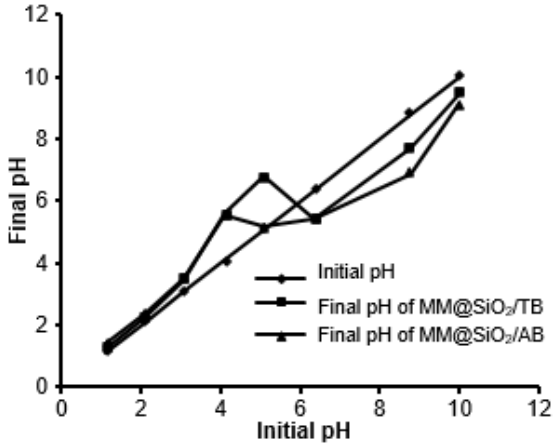

Fig 7. pH_{PZC} of MM@SiO_2/AB and MM@SiO_2/TB

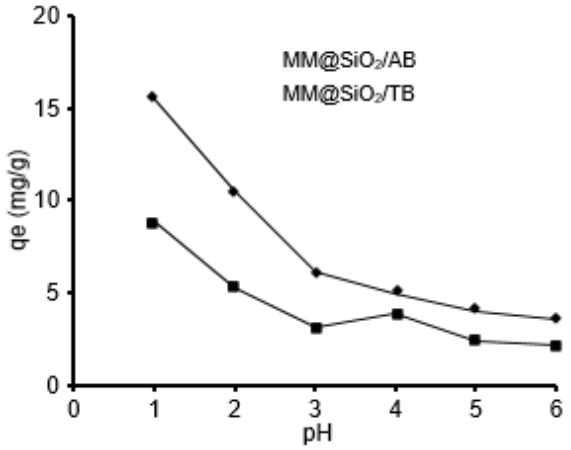

Fig 8. The effect of pH to adsorbed Au(III) on MM@SiO_2/AB and MM@SiO_2/TB

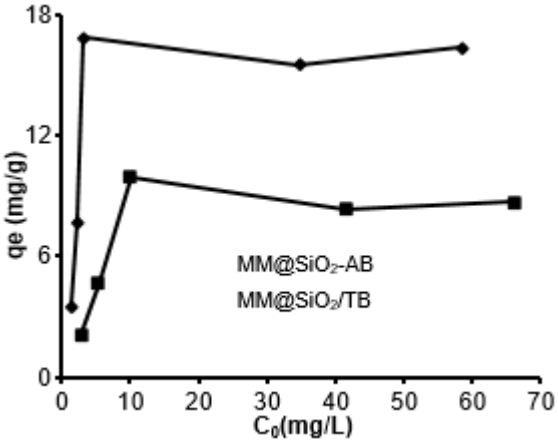

Fig 9. The effect of initial concentration on adsorbed Au(III) on MM@SiO_2/AB and MM@SiO_2/TB

is observed with the increase of solution pH (Fig. 8).

The highest amount of adsorbed Au(III) on both adsorbents is obtained at a pH of 1.0 with adsorption capacity of MM@SiO_2/AB is 15.58 mg/g while that of MM@SiO_2/TB is 8.88 mg/g. Those adsorbents show higher capacity in comparison to unmodified MM@SiO_2 2.61 mg/g at the range of pH tested. This optimum pH may be obtained since the amine groups on these adsorbents has been protonated perfectly so the amount of Au(III) that interact with the active sites of adsorbent increases. The adsorption capacity of MM@SiO_2/AB is greater than that of MM@SiO_2/TB. It is due to the higher of amine groups number on TB ligand which has the near distance between itself leads to steric hindrance when Au(III) adsorbed in high amount. Au(III) exist in solution as $[AuCl_4]^-$ when pH is below 3 [22] while coated MM positively charged at pH below theirs pH_{PZC}. This indicates that the Au(III) adsorption on MM@SiO_2/AB and MM@SiO_2/TB could be attributed to the electrostatic attraction. The positive charge of adsorbents surface increases with the decrease of pH. Thus the maximum adsorption capacity is obtained at lower pH and then the solution pH was set at 1.0 in the following experiments.

Adsorption isotherms

It is known that the maximum adsorption capacity of MM@SiO_2/AB and MM@SiO_2/TB is measured at the initial Au(III) concentration of 20 mg/L (Fig. 9). The Au(III) adsorption data on MM@SiO_2/AB and MM@SiO_2/TB were analyzed with Langmuir and Freundlich isotherm models. Langmuir adsorption isotherm model can be written as Eq. (3).

$$\frac{C_e}{q_e} = \frac{1}{q_{max}} C_e + \frac{1}{q_{max} K_L} \quad (3)$$

where q_e (mg/g) and C_e (mg/L) are the amount adsorbed and concentration of Au(III) at equilibrium, respectively, q_{max} is maximum adsorption capacity (mg/g) and K_L is Langmuir constant relating to the affinity of binding sites (L/mg). The values of q_{max} and K_L can be determined from the slope and intercept of C_e versus C_e/q_e plot. Freundlich adsorption isotherm empirically can be expressed in Eq. (4).

$$\ln q_e = \frac{1}{n} \ln C_t + \ln K_F \quad (4)$$

where K_F is Freundlich constant related to adsorption capacity of adsorbent and n is the Freundlich exponent related to adsorption intensity. The values of K_F and n can be calculated from the slope and intercept of ln C_t vs ln q_e plot.

Langmuir and Freundlich parameters and regression coefficient are shown in (Table 2). The linear regression coefficients (R^2) for the Langmuir model (more than 0.9823) are higher than that for Freundlich (less than 0.6036). Those values indicate that Au(III) adsorption on MM@SiO_2/AB and MM@SiO_2/TB fit with the Langmuir model and implied that the Au(III) adsorption on these adsorbent occurs in a single monolayer. Adsorption of Au(III) on these adsorbents have the q_{max} value of 17.15 mg/g for MM@SiO_2/AB and

that of 9.44 mg/g for MM@SiO_2/TB. These q_{max} values are higher than that for MM/SiO_2 (2.71 mg/g) showing the effect of coating MM with functional groups added. It may be understood because of two factors: firstly, the steric hindrance between Au(III) adsorbed. Secondly, the competition between $[AuCl_4]^-$ anion and Cl^- ion from the buffer solution to interact with active sites of adsorbent.

Adsorption kinetics

Adsorption kinetics is evaluated by varying contact time of Au(III) adsorption. The result shows that the adsorption of Au(III) is fast and reaches equilibrium within 45 min for both adsorbents (Fig. 10). Pseudo-first order and pseudo-second-order kinetic models are applied to evaluate the kinetics. Pseudo-first order and pseudo-second-order model are shown below.

$$\log (q_e - q_t) = \log q_e - \frac{k_1}{2.303} t \quad (5)$$

$$\frac{t}{q_t} = \frac{1}{q_e} t + \frac{1}{h} \quad (6)$$

$$k_2 = \frac{h}{q_e^2} \quad (7)$$

where q_e and q_t are the amounts of Au(III) adsorbed at equilibrium and time t, respectively; k_1 and k_2 are adsorption rate constant for pseudo-first-order and pseudo-second-order kinetics, respectively. The value of k_1 and k_2 can be obtained by plotting curves of t versus $\log(q_e-q_t)$ and t versus t/q_t.

Table 3 shows that Au(III) adsorption on MM@SiO_2/AB and MM@SiO_2/TB follows the kinetic model of pseudo-second order. The adsorption rate constant k_2 of Au(III) on MM@SiO_2/TB is higher than that on MM@SiO_2/AB. This indicates that the amount of Au(III) adsorbed on a constant mass of MM@SiO_2/TB at time unit is lower than that of MM@SiO_2/AB. From k_2 value, also known that MM@SiO_2/AB has a greater adsorption rate than MM@SiO_2/TB, as a result from inversely proportional to k_2 value. This result supported the kinetics models reported by previous researchers revealing that Au(III) adsorption on adsorbent follows pseudo-second-order with k_2 value in the order of 10^{-2} g/mg min [3,16].

Adsorption selectivity

Adsorption selectivity of Au(III) on MM@SiO_2/AB and MM@SiO_2/TB in metal ions mixture was conducted by adsorbing metal ions at constant Au(III) concentration

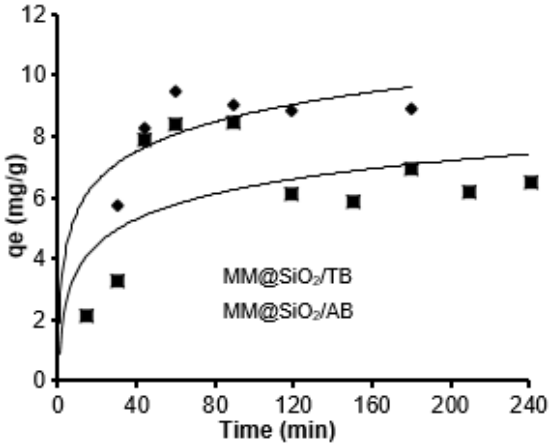

Fig 10. The effect of adsorption time to adsorbed Au(III) on MM@SiO_2/AB and MM@SiO_2/TB

Table 2. Adsorption isotherm parameters of Au(III) on MM@SiO_2/AB and MM@SiO_2/T

Adsorbent	Langmuir			Freundlich		
	q_{max} (mg/g)	K_L (L/mg)	R^2	K_F (mg/g)	n	R^2
MM@SiO_2/AB	17.15	0.33	0.9935	5.78	3.48	0.4959
MM@SiO_2/TB	9.44	0.19	0.9823	2.23	2.68	0.6036

Table 3. Adsorption kinetics parameters of Au(III) on MM@SiO_2/AB and MM@SiO_2/TB

Adsorbent	Pseudo first-order			Pseudo second-order		
	k_1 (min^{-1})	q_e (mg/g)	R^2	k_2 (g mg^{-1} min^{-1})	q_e (mg/g)	R^2
MM@SiO_2/AB	1.38×10^{-2}	1.79	0.6503	1.16×10^{-2}	9.52	0.9884
MM@SiO_2/TB	1.15×10^{-3}	1.42	0.0061	1.46×10^{-2}	6.83	0.9486

Table 4. Selectivity of MM@SiO_2/AB and MM@SiO_2/TB for Au(III) adsorption toward Cu(II) and Ni(II)

Adsorbent	Initial concentration (mg/L)			D (L/g)			$\alpha_{Au/Cu}$	$\alpha_{Au/Ni}$
	Au(III)	Cu(II)	Ni(II)	Au(III)	Cu(II)	Ni(II)		
MM@SiO_2/AB	20	20	20	53.67	1.52	2.64	35.21	20.36
	20	20	40	36.27	1.60	2.72	22.67	13.33
	20	20	60	34.65	1.52	2.87	22.73	12.07
	20	40	20	13.39	1.46	2.20	9.14	6.09
	20	60	20	13.91	1.32	2.48	10.91	5.61
MM@SiO_2/TB	20	20	20	12.16	2.68	2.01	4.53	6.05
	20	20	40	11.36	2.68	1.98	4.23	5.74
	20	20	60	7.00	2.78	2.17	2.52	3.22
	20	40	20	13.07	2.21	1.52	5.90	8.60
	20	60	20	18.42	1.85	1.74	9.98	10.57

Table 5. Percentage of metal ion desorbed in a mixture of Au(III), Cu(II) and Ni(II)

Adsorbent	Initial concentration (mg/L)			Adsorbed metal ion (mg/g)			Desorbed metal ion (mg/g)			Desorbed metal ion (%)		
	Au(III)	Cu(II)	Ni(II)	Au(III)	Cu(II)	Ni(II)	Au(III)	Cu(II)	Ni(II)	Au(III)	Cu(II)	Ni(II)
MM@SiO_2/AB	20	0	0	17.00	0.00	0.00	12.37	0.00	0.00	72.76	0.00	0.00
	20	20	20	14.37	13.03	13.94	9.85	0.31	0.90	68.56	2.38	6.47
	20	40	20	17.65	12.97	17.95	9.45	0.79	0.80	53.56	6.09	4.48
	20	20	40	17.78	16.48	11.29	9.45	0.25	0.40	53.15	1.53	3.56
MM@SiO_2/TB	20	0	0	9.26	0.00	0.00	6.55	0.00	0.00	70.74	0.00	0.00
	20	20	20	17.67	16.88	17.23	14.25	1.11	1.96	80.61	6.58	11.37
	20	40	20	17.90	36.52	12.71	11.93	0.45	2.16	66.63	1.24	16.99
	20	20	40	17.66	15.35	36.62	12.58	0.54	2.25	71.25	3.53	6.15

and various other metal ion concentrations. Adsorption selectivity is presented as a selectivity coefficient (coefficient distribution ratio of Au(III) to another ion) and calculated using Eq. (1).

From Table 4 could be known that the selectivity of Au(III) on MM@SiO_2/AB and MM@SiO_2/TB toward Cu(II) and Ni(II) is higher than 1. It proves that these adsorbents adsorb Au(III) selectively toward other metals ion in the mixture. This is caused by the tendency of MM@SiO_2/AB and MM@SiO_2/TB to interact with $[AuCl_4]^-$ anion electrostatically than with Cu(II) and Ni(II) resulting in electrostatic repulsion. It can be seen that adsorption on MM@SiO_2/AB gives greater selectivity coefficient of Au(III) than that on MM@SiO_2/TB. This result is agreed with the adsorption data of Au(III) in a single metal ion system which MM@SiO_2/AB has a higher capability to adsorbing Au(III).

Desorption

Desorption of Au(III), Cu(II) and Ni(II) metal ions from MM@SiO_2/AB and MM@SiO_2/TB was investigated by varying the concentration of Cu(II) and Ni(II) adsorbed on adsorbents while Au(III) concentration was made constant. A solution of 1 M thiourea in 1 M HCl has been reported to yield the high percentage recovery of gold and the least dissolution of magnetic material particles [23].

Table 5 represents that desorption of Au(III) from MM@SiO_2/AB and MM@SiO_2/TB result the high percentage of Au(III) desorbed (more than 53.15%) and this value is higher than the percentage of Cu(II) and Ni(II) desorbed (less than 16.99%). Based on hard-soft-acid-base (HSAB) theory, Au(III) as soft acid, could interact with S of thiourea as a soft base through sharing of electrons involving covalent forces. This covalent

bonding results in a stable complex between thiourea and Au(III) so that Au(III) tends to bind with thiourea than with amine groups on adsorbents surface. This phenomenon does not occur on Cu(III) and Ni(II) as intermediate acid (borderline) thus the amount of Cu(II) and Ni(II) desorbed is lower than that of Au(II).

■ CONCLUSION

It can be concluded that 2-aminobenzimidazole and 1-(o-tolyl)biguanide modified silica have been successfully coated on the iron sand magnetic material using CPTS as a cross-linking agent. The Au(III) adsorption capacity of MM@SiO_2/AB and that of MM@SiO_2/TB are higher than that of MM/SiO_2. The adsorption of Au(III) on these adsorbents in single metal ion system fit Langmuir isotherm model and follow pseudo-second-order reaction. The selectivity adsorption test proves that MM@SiO_2/AB and MM@SiO_2/TB have high selectivity towards Au(III) in a mixture of Au(III), Cu(II) and Ni(II). The desorption metal ions from adsorbents show that percentage of Au(III) adsorbed is higher than that of Cu(II) and that of Ni(II).

■ ACKNOWLEDGMENTS

This work was funded by the Ministry of Research, Technology and Higher Education of Indonesia through research grant of *Penelitian Berbasis Kompetensi (PBK)*, contract number: 1731/UN1/DITLIT/DIT-LIT/LT/2018.

■ REFERENCES

[1] Shabbir, S., Lee, Y., and Rhee, H., 2015, Au(III) catalyst supported on a thermoresponsive hydrogel and its application to the A-3 coupling reaction in water, *J. Catal.*, 322, 104–108.

[2] Kim, E.Y., Kim, M.S., Lee, J.C., and Pandey, B.D., 2011, Selective recovery of gold from waste mobile phone PCBs by hydrometallurgical process, *J. Hazard. Mater.*, 198, 206–215.

[3] Firlak, M., Yetimoğlu, E.K., and Kahraman, M.V., 2014, Adsorption of Au(III) ions from aqueous solutions by thiol-ene photoclick hydrogels and its application to electronic waste and geothermal water, *J. Water Process Eng.*, 3, 105–116.

[4] Arshadi, M., and Mousavi, S.M., 2015, Enhancement of simultaneous gold and copper extraction from computer printed circuit boards using *Bacillus megaterium*, *Bioresource Technol.*, 175, 315–324.

[5] Aguado, J., Arsuaga, J.M., Arencibia, A., Lindo, M., and Gascón, V., 2009, Aqueous heavy metals removal by adsorption on amine-functionalized mesoporous silica, *J. Hazard. Mater.*, 163 (1), 213–221.

[6] Sakti, S.C.W., Narita, Y., Sasaki, T., Nuryono, and Tanaka, S., 2015, A novel pyridinium functionalized magnetic chitosan with pH-independent and rapid adsorption kinetics for magnetic separation of Cr(VI), *J. Environ. Chem. Eng.*, 3 (3), 1953–1961.

[7] Behbahani, M., Najafi, F., Amini, M.M., Sadeghi, O., Bagheri, A., and Hassanlou, P.G., 2014, Solid phase extraction using nanoporous MCM-41 modified with 3,4-dihydroxybenzaldehyde for simultaneous preconcentration and removal of gold(III), palladium(II), copper(II) and silver(I), *J. Ind. Eng. Chem.*, 20 (4), 2248–2255.

[8] Li, X., Zhang, C., Zhao, R., Lu, X., Xu, X., Jia, X., Wang, C., and Li, L., 2013, Efficient adsorption of gold ions from aqueous systems with thioamide-group chelating nanofiber membranes, *Chem. Eng. J.*, 229, 420–428.

[9] Araghi, S.H., and Entezari, M.H., 2015, Amino-functionalized silica magnetite nanoparticles for the simultaneous removal of pollutants from aqueous solution, *Appl. Surf. Sci.*, 333, 68–77.

[10] Fotoohi, B., and Mercier, L., 2015, Some insights into the chemistry of gold adsorption by thiol and amine functionalized mesoporous silica in simulated thiosulfate system, *Hydrometallurgy*, 156, 28–39.

[11] Sakti, S.C.W., Siswanta, D., and Nuryono, 2013, Adsorption of gold(III) on ionic imprinted amino-silica hybrid prepared from rice hull ash, *Pure Appl. Chem.*, 85 (1), 211–223.

[12] Hastuti, S., Nuryono, and Kuncaka, A., 2015, L-Arginine-modified silica for adsorption of gold(III), *Indones. J. Chem.*, 15 (2), 108–115.

[13] Ebrahimzadeh, H., Tavassoli, N., Amini, M.M., Fazaeli, Y., and Abedi, H., 2010, Determination of

very low levels of gold and palladium in wastewater and soil samples by atomic absorption after preconcentration on modified MCM-48 and MCM-41 silica, *Talanta*, 81 (4-5), 1183–1188.

[14] Zhang, Y., Xu, Q., Zhang, S., Liu, J., Zhou, J., Xu, H., Xiao, H., and Li, J., 2013, Preparation of thiol-modified Fe_3O_4@SiO_2 nanoparticles and their application for gold recovery from dilute solution, *Sep. Purif. Technol.*, 116, 391–397.

[15] Alizadeh, A., Khodaei, M.M., Beygzadeh, M., Kordestani, D., and Feyzi, M., 2012, Biguanide-functionalized Fe_3O_4/SiO_2 magnetic nanoparticles: An efficient heterogeneous organosuperbase catalyst for various organic transformations in aqueous media, *Bull. Korean Chem. Soc.*, 33 (8), 2546–2552.

[16] Nuryono, N., Muliaty, E., Rusdiarso, B., Sakti, S.C.W., and Tanaka, S., 2014, Adsorption of Au(III), Cu(II) and Ni(II) on magnetite coated with mercapto groups modified rice hull ash silica, *J. Ion Exch.*, 25 (4), 114–121.

[17] Nuryono, N., Rosiati, N.M., Rusdiarso, B., Sakti, S.C.W., and Tanaka, S., 2014, Coating of magnetite with mercapto modified rice hull ash silica in a one-pot process, *SpringerPlus*, 3, 515.

[18] Fahmiati, Nuryono, and Suyanta, 2017, Characteristics of iron sand magnetic material from Bugel beach, Kulon Progo, Yogyakarta, *IOP Conf. Ser. Mater. Sci. Eng.*, 172 (1), 012020.

[19] Sui, D.P., Chen, H.X., Liu, L., Liu, M.X., Huang, C.C., Fan, H.T., 2016, Ion-imprinted silica adsorbent modified diffusive gradients in thin films technique: Tool for speciation analysis of free lead species, *Talanta*, 148, 285–291.

[20] Azmiyawati, C., Nuryono, and Narsito, 2014, Synthesis of disulfonato-silica hybrid from rice husk ash, *JOMB*, 3 (4), 301–305.

[21] Lin, Y.F., Chen, H.W., Chien, P.S., Chiou, C.S., and Liu, C.C., 2011, Application of bifunctional magnetic adsorbent to adsorb metal cations and anionic dyes in aqueous solution, *J. Hazard. Mater.*, 185 (2-3), 1124–1130.

[22] Pacławski, K., and Fitzner, K., 2004, Kinetics of gold(III) chloride complex reduction using sulfur(IV), *Metall. Mater. Trans. B*, 35 (6), 1071–1085.

[23] Kraus, A., Jainae, K., Unob, F., and Sukpirom, N., 2009, Synthesis of MPTS-modified cobalt ferrite nanoparticles and their adsorption properties in relation to Au(III), *J. Colloid Interface Sci.*, 338 (2), 359–365.